Ab-initio Study of new materials from high pressure

Thesis submitted for the degree of
Magister Philosophæ

Candidate:
Javier A. Montoya M.

Supervisors:
Prof. Sandro Scandolo
Dr. Roger Rousseau

Sector of
Condensed matter Theoretical
and computational physics

Contents

List of Figures

Chapter 1

Introduction

Many important achievements have been obtained by modern solid state physics in the description of the vibrational properties of solids. Model theories of lattice dynamics [1] reached the state in which experimental values can be reproduced with great accuracy by fitting the parameters of the model to experiments. However, these last years have seen increased demand for "parameter-free"approaches, both for the intrinsic theoretical interest and for the fundamental role played when the experimental information is lacking or debated.

The first part of the present thesis is inspired by the experimental results obtained at the Geophysical Laboratory, Carnegie Institution of Washington by Eugene Gregoryanz *et al.* [2]. The scientific group managed to synthesize Platinum nitride at high pressure and temperature, the new compound was quenched to atmospheric pressure and room temperature and then characterized by Raman spectroscopy, in situ X-ray diffraction and Synchrotron X-ray diffraction, among many other experimental techniques. At least to our knowledge, no Ab-initio characterization of this system has been made so far. An accurate ab-initio study of this new material could be helpful on clarifying its structural properties. A second problem treated in this thesis is the one related with the prediction of a polymeric phase for CO_2 under less extreme conditions than the ones reported experimentally so far, by running ab-initio molecular dynamics simulations on a transition metal-doped CO_2 system at increasing pressures.

Thus, our aim in this work will be precisely to use one of those parameter-free approaches mentioned in the first paragraph, namely, the Density Functional Theory (DFT) in order to simulate the behavior of a given crystalline periodic system. Some theoretical background concerning Molecular Dynamics and the DFT techniques, as well as some details on the specific set of computer programs (*espresso*) used for this work are discussed in *Chapters 2* and *3*.
C*hapter 4* treats specific aspects concerning the physical implications of working at high pressures and hence it clarifies its use as a method for synthesizing new compounds.
C*hapters 5* and *6* are devoted to the analysis and discussion of the outcomes that were obtained when applying these techniques to our two particular problems.
Finally, *Chapter 7* presents the conclusions and perspectives of this work.

Chapter 2

Molecular Dynamics (MD) and first-principles calculations

2.1 MD

Molecular dynamics simulation is a technique for computing the equilibrium and transport properties of a classical many body system. In this context, the word classical means that the nuclear motion of the constituent parts obeys the laws of classical mechanics. This is an excellent approximation for a wide range of materials. Only when we consider the translational or rotational motion of light atoms or molecules (He, H2, D2) or vibrational motion with frequency ν such that $h\nu$ k_B T should we worry about quantum effects.

The idea behind molecular dynamics simulations is to enable us to mimic real experiments, in this sense we proceed in the same way in both cases; first we prepare a sample of the material that we want to study, we set a mechanism for measuring observable quantities (e.g., a thermometer, manometer, viscometer, etc) and we establish a sampling rate for measuring those quantities. The system evolves following Newton's equations and since some time for equilibration is requires, the more we let the system run the best are the statistics that we will get from our simulations an this will allow better estimations of the measured quantities.
To measure an observable quantity in a Molecular Dynamics simulation, we must first of all be able to express this observable as a function of the positions and momenta of the particles in the system. For instance, a convenient definition of temperature in a classical many body system makes use of the equipartition theorem. Thus, we have:

$$\left\langle \frac{mv_\alpha^2}{2} \right\rangle = \frac{k_B T}{2} \tag{2.1}$$

In a simulation, we use this equation as an operational definition of the temperature. In practice, we would measure the total kinetic energy of the system

and divide this by the number of degrees of freedom N_f. As the total kinetic energy of a system fluctuates, so does the instantaneous temperature:

$$T(t) = \sum_i \left(\frac{m v_i^2(t)}{k_B N_f} \right) \tag{2.2}$$

The relative fluctuations in the temperature will be of the order $(\frac{1}{\sqrt{N_f}}$. As N_f is typically on the order of $10^2 - 10^3$, the statistical fluctuations in the temperature are on the order of 5-10% . To get an accurate estimate of the temperature, one should average over many fluctuations.

A typical MD program is constructed as follows:

1. We read in the parameters that specify the starting conditions of the run.

2. We compute the forces on all particles.

3. We integrate Newton's equations of motion. This step and the previous one make up the core of the simulation and are repeated until we are satisfied with the equilibration + measuring time needed for our statistic averages.

4. After completion of the central loop (steps 2 and 3) we conclude computing and printing the average of measured quantities, and stop.

2.2 Ab-inito calculations

Ab-inito or first-principles calculations consist on the complete treatment of the quantum mechanical problem. In the following sections however, we will see that this is not always possible in practice but the problem still can be addressed by imposing reasonable approximations to the full problem.

2.2.1 The Crystal Hamiltonian

First of all we will describe the crystal Hamiltonian, that is the one which in principle contains all the physics of the many body system and from the solution of which, we would like to derive all the observable quantities. It is:

$$\begin{aligned} \mathrm{H} = & \sum_i \left(-\frac{\hbar^2}{2m} \nabla_i^2 \right) + \sum_\alpha \left(-\frac{\hbar^2}{2M_\alpha} \nabla_\alpha^2 \right) + \\ & \frac{1}{2} \sum_{i \neq j} \frac{e^2}{r_{ij}} + \frac{1}{2} \sum_{\alpha \neq \beta} \frac{Z_\alpha Z_\beta e^2}{R_{\alpha\beta}} - \sum_{i,\alpha} \frac{Z_\alpha e^2}{|r_i - R_\alpha|}. \end{aligned} \tag{2.3}$$

The first term is the electronic kinetic energy, being m the electronic mass and ∇_i^2 the Laplacian acting over the electronic coordinates $\{r_i\}$. The second term is the energy corresponding to the motion of the nuclei, where M_α is the nuclear mass and ∇_α^2 is the Laplacian acting over the nuclear coordinates $\{R_\alpha\}$.

The third and fourth terms are the pairwise electrostatic electron-electron and nucleus-nucleus interactions respectively, where: $r_{ij} = |r_i - r_j|$ and $R_{\alpha\beta} = |R_\alpha - R_\beta|$ are the electron-electron and nucleus-nucleus separations of the pairs which are being considered and Z_α represents the charge of the αth nucleus. Finally, the fifth term corresponds to the electron-nuclei attraction.

From the Hamiltonian given above, is clear that the number of independent variables in the corresponding Schröinger's equation is determined by the number of particles involved (which for a macroscopic crystal is of the order of $10^{23} cm^{-3}$). Therefore, a direct solution for such kind of equation is not possible. Hence when dealing with this kind of problems, people very often try to work them out by doing different successive approximations which sometimes may compromise the accuracy of the final result, or whose results are not so general, working then for only a few types of systems.

Very frequently the first of those approximations that people do is the adiabatic (or *Born-Oppenheimer* [4]) approximation. This is not very critical in terms of loss of accuracy, and simplifies considerably the problem so we will explain it.

2.2.2 The Born-Oppenheimer approach

If we divide the system into light particles (electrons) and heavy ones (atomic nuclei), in thermodynamic equilibrium the mean value for the kinetic energy of both kind of particles is of the same order but, due to the big mass difference between protons+neutrons and electrons, the electronic velocities are much faster than the nuclear ones (approximately two orders of magnitude). Then, for every modification in the position of the atomic nuclei an almost instantaneous rearrangement of the electrons occurs, following the new nuclear positions. This allows us to consider, at least to a first approximation, the movement of the electrons as if they were in an irrotational field due to *fixed* nuclei. While studying the movement of the nuclei, by the contrary, only the potential originated by the mean electronic spatial distribution (and not the instantaneous one) must be taken into account. Is this kind of approach which is known as the *adiabatic* or *Born-Oppenheimer approximation.*

Within this approximation the Schröinger's equation can be rewritten as:

$$\left(-\sum_\alpha \frac{\hbar^2}{2M_\alpha} \nabla_\alpha^2 + E_0(R) \right) \Phi(R) = \varepsilon \Phi(R) \tag{2.4}$$

being $R \equiv \{R_\alpha\}$ the set of all the nuclear coordinates and $E_0(R)$ the clamped-ion energy of the system, which is often referred to as the *Born-Oppenheimer energy surface.* In practice, $E_0(R)$ is the ground state energy of a system of interacting electrons moving in the field of fixed nuclei, which obeys the Schröinger's equation $H_{BO}(R)\varphi_n = E_n(R)\varphi_n$ where the Hamiltonian —which acts onto the electronic variables and depends only parametrically upon R— reads

$$H_{BO}(R) = -\frac{\hbar^2}{2m} \sum_i \nabla_i^2 + \frac{e^2}{2} \sum_{i \neq j} \frac{1}{r_{ij}} + \frac{e^2}{2} \sum_{\alpha \neq \beta} \frac{Z_\alpha Z_\beta}{R_{\alpha\beta}} - \sum_{i,\alpha} \frac{Z_\alpha e^2}{|r_i - R_\alpha|}. \tag{2.5}$$

This could be simply taken as a rearrangement of the equation 2.3, but it is important to notice that now the electronic part is decoupled from the rest and can be solved independently, using the set of nuclear positions R, only as parameters.

2.2.3 Linear response

From the ground state solution for the electronic Hamiltonian (equation 2.5) for every R, we are able to obtain the mentioned energy surface $E_0(R)$ which enters into the nuclear Schröinger's equation (equation 2.4), thus determining the nuclear behavior.

Since the works of De Cicco and Johnson [5] and of Pick, Cohen and Martin [6], it is well known that the harmonic force-constants of crystals are determined by their static linear response, establishing connections between the dynamical matrices and the electronic properties of the material. Making use of the formalism just developed in the previous subsection, we can note that the equilibrium geometry of the system is given by the condition that the forces acting on individual nuclei vanish:

$$F_\alpha = -\frac{\partial E_0(R)}{\partial R_\alpha} = 0. \tag{2.6}$$

Whereas the vibrational frequencies ω are determined by the eigenvalues of the Hessian of the Born-Oppenheimer energy, scaled by the nuclear masses

$$det \left| \frac{1}{\sqrt{M_\alpha M_\beta}} \frac{\partial^2 E_0(R)}{\partial R_\alpha \partial R_\beta} - \omega^2 \right| = 0. \tag{2.7}$$

The calculation of the equilibrium geometry and of the vibrational properties of a system thus amounts to computing the first and second derivatives of its Born-Oppenheimer energy surface.

2.2.4 Ab-initio MD

The calculation of the force acting on every particle is the most time-consuming part of almost all Molecular Dynamics simulations. For the most simple case of pair-wise inter-atomic forces, the time needed for the evaluation of these forces scales as N^2. In ŕealäpplications of the MD technique more sophisticated and time-expensive algorithms for the analytical calculation of the forces are used, they include many body terms and parameters that have to be fitted to experiments. Those algorithms tend to be very precise, but are tunned for determined coordination numbers, pressures, temperatures and other environmental parameters that the researcher could like to change during the simulation. Then a parameter free algorithm for the force calculations become desirable, this is achieved by the Ab-initio Molecular Dynamics technique which uses atomic forces calculated from first principles, with no dependence on the material. This is possible only from a full quantum mechanical treatment of the problem and is in this aspect were the Density Functional Theory together with the concepts already seen in this chapter play a main role.

Chapter 3

Density Functional Theory

The fundamental tenet of density functional theory is that any property of a system of many interacting particles can be viewed as a functional of the ground state density $n_0(r)$; that is, one scalar function of position $n_0(r)$, in principle, determines all the information in the many-body wave functions for the ground state and all excited states. The existence proofs for such functionals, given in the original works of Hohenberg and Kohn [7] and of Mermin [8], are disarmingly simple. However, they provide no guidance whatsoever for constructing the functionals, and no exact functionals are known for any system of more than one electron.

Density Functional Theory (DFT) would remain a minor curiosity today if it were not for the ansatz made by Kohn and Sham [9], which has provided a way to make useful, approximate ground state functionals for real systems of many electrons. The Kohn-Sham ansatz replaces the interacting many-body problem with an auxiliary independent particle problem with all many body effects included in an exchange-correlation functional. This is an ansatz that, in principle, leads to *exact* calculations of properties of many-body systems using independent particle methods —even though nobody until now knows the exact formulation for the functional which has to be minimized— and has made possible approximate formulations that have proved to be remarkably successful. In the present work we used the Local Density Approximation (LDA), which is one of those successful, practical but approximate, formulations for the exchange-correlation functional (being this the crucial part in the Kohn-Sham approach as we will see) and allow us to obtain good ground state dynamic properties such as phonon modes, bulk modulus, etc. During the following sections of this chapter we will try to go deeper into the details and motivations of this technique.

3.1 Force theorem

An extra advantage of the adiabatic approximation is that due to the assumption that the electrons equilibrate very fast after a nuclear movement, we can think of them as being always in a steady state which is the fundamental condition for the Hellmann-Feynman force-theorem [11, 12] to be valid.

The force theorem states that the *first* derivative of the eigenvalues of a Hamiltonian, H_λ, that depends on a parameter λ is given by the expectation value of the derivative of the Hamiltonian, so it can be used in the following way

$$\frac{\partial E_\lambda}{\partial \lambda} = \left\langle \Psi_\lambda \left| \frac{\partial H_\lambda}{\partial \lambda} \right| \Psi_\lambda \right\rangle \tag{3.1}$$

where Ψ_λ is the eigenfunction of H_λ corresponding to the E_λ eigenvalue: $H_\lambda \Psi_\lambda = E_\lambda \Psi_\lambda$. Remembering now that, in the Born-Oppenheimer approximation, nuclear coordinates act as parameters in the electronic Hamiltonian, $H_{BO}(R)$, whose ground state determines the energy surface $E_0(R)$ appearing in the Schröinger's equation for the nuclei; the force acting on the Ith nucleus will then be

$$F_\alpha = -\frac{\partial E_0(R)}{\partial R_\alpha} = \left\langle \varphi_0(r,R) \left| \frac{\partial H_{BO}(R)}{\partial R_\alpha} \right| \varphi_0(r,R) \right\rangle \tag{3.2}$$

where $\varphi_0(r,R)$ is the electronic ground-state wave function of the Born - Oppenheimer Hamiltonian[1] being $r \equiv \{r_i\}$ the set of all the electronic coordinates. This Hamiltonian depends on R via the electron-nucleus interaction that couples to the electronic degrees of freedom only through the electron charge density. The Hellman-Feynman theorem states in this case that

$$F_\alpha = \underbrace{\int n_R(r) \frac{\partial}{\partial R_\alpha} \overbrace{\left(\sum_{i,\alpha} \frac{Z_\alpha e^2}{|r_i - R_\alpha|} \right)}^{V_R(r)} dr}_{e^- - \textit{nucleus interaction}} - \underbrace{\frac{\partial}{\partial R_\alpha} \overbrace{\left(\frac{e^2}{2} \sum_{\alpha \neq \beta} \frac{Z_\alpha Z_\beta}{R_{\alpha\beta}} \right)}^{E_N(R)}}_{\textit{completely nuclear part}} \tag{3.3}$$

where $n_R(r)$ is the ground-state electron charge density corresponding to the nuclear configuration R and the completely-nuclear part is just a number which can be calculated exactly for each of those configurations. The Hessian of the Born-Oppenheimer energy surface appearing in equation 2.7 is thus, obtained by differentiating the Hellmann-Feynman forces with respect to nuclear coordinates,

$$\frac{\partial^2 E_0(R)}{\partial R_\alpha \partial R_\beta} \equiv -\frac{\partial F_\alpha}{\partial R_\beta} = \int \frac{\partial n_R(r)}{\partial R_\beta} \frac{\partial V_R(r)}{\partial R_\alpha} dr + \int n_R(r) \frac{\partial^2 V_R(r)}{\partial R_\alpha \partial R_\beta} dr + \frac{\partial^2 E_N(R)}{\partial R_\alpha \partial R_\beta}. \tag{3.4}$$

3.1.1 Density as basic variable

The last equation states that the calculation of the Hessian of the Born - Oppenheimer energy surfaces requires the calculation of the ground-state electron charge density $n_R(r)$ as well as its *linear response* to a distortion of the nuclear geometry, $\partial n_R(r)/\partial R_\alpha$. The Hessian matrix is usually called the *matrix of the interatomic force constants* or simply the *dynamical matrix*. An important fact related with these matrices that will be used by our computer program is that, within the adiabatic approximation, the lattice distortion associated with

[1] We will always assume during the ab-initio calculations of this work that we are at T=0 K, i.e. in the ground state.

a phonon can be seen simply as a static perturbation acting on the electrons, showing again the connection between the dynamical and electronic properties of the material and making also easier the phonon calculations. These fundamental results, as mentioned at the beginning of this section, were first stated in the late 1960s by De Cicco and Johnson in (1969) and by Pick, Cohen and Martin in (1970).
According to the preceding discussion, the calculation of the derivatives of the Born-Oppenheimer energy surface with respect to the nuclear coordinates requires *only* a knowledge of the *electronic charge-density distribution.* This fact is nothing else than a special case of a much more general property of the systems of interacting electrons, known as the *Hohenberg and Kohn (1964) theorem.*

3.2 The Hohenberg-Kohn theorem

According to the Hohenberg-Kohn theorem [7], no two different potentials (different up to a constant) acting on the electrons of a given system can give rise to a same ground-state electronic charge density. The prove is quite simple and follows after a Reductio-ad-Absurdum:

Let us assume that there are two external potentials $V_1(r)$ and $V_2(r)$ which differ by more than a constant and which lead the same ground-state electronic density. Then if we consider H_1 as being the Hamiltonian corresponding to $V_1(r)$ with Ψ_1 being the ground-state wave function associated with this Hamiltonian, and assuming equivalent definitions for $V_2(r)$, then follows that:

$$E_1 = \langle \Psi_1 | H_1 | \Psi_1 \rangle < \langle \Psi_2 | H_1 | \Psi_2 \rangle, \tag{3.5}$$

we are here assuming that these are non-degenerate ground states so that, the inequality holds as stated in the previous formula. Now, using this expression and rearranging some terms:

$$\begin{aligned} \langle \Psi_2 | H_1 | \Psi_2 \rangle &= \langle \Psi_2 | H_2 | \Psi_2 \rangle + \langle \Psi_2 | H_1 - H_2 | \Psi_2 \rangle \\ &= E_2 + \int [V_1(r) - V_2(r)] n_R^0(r) dr, \end{aligned} \tag{3.6}$$

so that

$$E_1 < E_2 + \int [V_1(r) - V_2(r)] n_R^0(r) dr. \tag{3.7}$$

On the other hand if we consider E_2 in exactly the same way, we find the same kind of equation, with subscripts 1 and 2 interchanged,

$$E_2 < E_1 + \int [V_2(r) - V_1(r)] n_R^0(r) dr. \tag{3.8}$$

And finally, if we add together (3.7) and (3.8), we arrive at the contradictory inequality $E_1 + E_2 < E_1 + E_2$, which establishes the desired result: *there cannot be two different external potentials differing by more than a constant which give rise to the same non-degenerate ground state charge density. Then, the density uniquely determines the external potential within a constant.*

This theorem provides the foundation of what is currently known as *density-functional theory* (DFT; Parr and Yang [14], 1989; Dreizler and Gross [15], 1990). It allows an enormous conceptual simplification of the ground-state properties of a system of interacting electrons, for it replaces the traditional description based on wave functions (which depend on $3N$ independent variables, N being the number of electrons) with a much more tractable description in terms of the charge density, which depends on only three variables.

To see this, let us take the ion-ion interaction energy ($E_N(R)$ in equation 3.3) as a reference point, then we are left with the following expression which is the one that has to be minimized in order to obtain the ground-sate energy and electronic density distribution:

$$E[n_R] = F[n_R] + \int n_R(r)V(r)dr. \tag{3.9}$$

Here we see that (as in equation 3.3) $V(r)$ is the external potential acting over the electronic charge density due to the ions and is the remaining part (the one represented by $F[n_R]$), which offers major difficulties. In fact there are two main problems: the first is that Hohenberg and Kohn didn't provide an exact form for the $F[n_R]$ functional, and the second is that the conditions to be fulfilled for a function n_R to be considered an acceptable ground state charge distribution (and hence domain of the functional F) are poorly characterized. About the last problem, one usually has to be content to impose the proper normalization of the charge density by the use of a Lagrange multiplier; and about the first problem, that is exactly what Kohn and Sham tried to address so in the next section we will give a short description of what they did.

3.3 The Kohn-Sham ansatz

As mentioned in the previous section, the Hohenberg and Kohn theorem, states that all the physical properties of a system of interacting electrons are uniquely determined by its ground-state charge density distribution. This property holds independently of the precise form of the electron-electron interaction. In particular when the strength of this interaction vanishes, the energy functional defines the ground state kinetic energy of a system of noninteracting electrons, which can be used as a limiting case or starting point for the construction of a general functional. This fact was used by Kohn and Sham [9], to map the problem of a system of interacting electrons onto an equivalent noninteracting problem. To this end, the unknown energy functional can be cast in the form

$$F[n_R] = T_0[n_R] + \frac{e^2}{2}\int \frac{n_R(r)n_R(r')}{r-r'}drdr' + E_{xc}[n_R] \tag{3.10}$$

where $T_0[n_R]$ is the mentioned kinetic energy functional for a system of noninteracting electrons having a density $n_R(r)$, the second term is the classical electrostatic self-interaction of the electron charge-density distribution (also called *Hartree* term) and finally a new quantity, $E_{xc}[n_R]$, is defined and represents the so called *exchange-correlation energy*. The only really unknown quantity is

this exchange-correlation energy functional[2] and, in principle, the quality of the solution of the full many body problem will be only limited by the quality of the approximation used for it.

In the weakly inhomogeneous case, where the deviation of the density is small from its homogeneous value, Kohn and Sham proposed that the exchange-correlation energy can be written as

$$E_{xc}[n_R] = \int n_R(r)\epsilon_{xc}[n_R(r)]dr \tag{3.11}$$

where $\epsilon_{xc}[n_R(r)]$ is the exchange-correlation energy per particle of a homogeneous system of density n. This approximation implies that an inhomogeneous system is replaced by a piece-wise homogeneous system; precisely coming from this reason is that this *ansatz*, is called the *local density approximation* (LDA), which has been proved to demonstrate the outstanding of the DFT, even when applied to not very homogeneous systems.

3.4 Plane waves and pseudopotentials

Even with such a big help coming from the simplification mentioned in section 2.2.2 and from the power of the Hohenberg-Kohn theorem plus the Kohn Sham ansatz; the many body problem is still very difficult to solve because if we want to be precise, we should take into account the field of the bare nuclei and consider the motion of *all* the electrons. This involves too many particles and would give place to extremely long computational times in the sense that it is very difficult to find a nice type of function which fulfills the conditions of: matching the Kohn-Sham electronic density accurately everywhere and making the energy-minimization process easy for standard computer algorithms.

In order to get a further reduction in the computational effort required for the calculation, but still taking into account the physics of the problem, people define periodic boundary conditions therefore imagining the system as an infinite crystal. This offers the possibility of thinking the electronic density as a superposition of plane waves, where the size of the plane-wave basis set used for each particular problem can be easily tuned by defining an energy cutoff that automatically will limit the number of components we are able to use. Then, the goal of this approach is to perform an "easy"calculation by using the minimum possible amount of plane waves for constructing the electronic density, but without compromising the accuracy. This should work fine for outer (mainly delocalized) electrons but, for the inner electrons, the electronic densities would be more accurately modeled if they were worked out through the superposition of atomic wave functions. This is due to the fact that those electrons are much more localized and in a plane-wave scheme they would need a much bigger set of wave functions to be represented accurately.

It is because of this problem that another well known and very common approximation, called the *valence approximation*, is also used. This relies on considering

[2]Because the energy coming from $T_0[n_R]$ can be obtained in an indirect way, see for example [13].

that all the interesting physical properties of the atoms in a crystal are mostly due to the valence electrons. Under this approximation we will take the core electrons as entities which are merged with the nucleus in an ion-like structure. Those *ions* can then be placed as genuine building blocks of the crystal because after being conveniently modeled, using a suitable basis set, they (or at least the main features acting over their valence electrons and which affects their surface and bonding properties) can be effectively represented through the so-called *pseudopotentials* [20, 21, 22, 23] which are artificial, effective and norm-conserving potentials that, in addition, can be constructed to fit perfectly in our plane-wave scheme. Of course when constructing pseudopotentials we are free to decide how many electrons will be considered core ones and how many will be on the valence region. Even though this differentiation is quite standard however, the construction of pseudopotentials is an art by itself, and the most recommended thing to do is to use the well done and tested ones that are already available in the Internet in sites as *www.democritos.it.*[3].

3.5 The ESPRESSO package

Ab-initio methods based on Density-Functional Theory (DFT) are by now common and well established tools for studying structural and vibrational properties of materials on very realistic grounds. The plane-wave pseudopotential method and the Local-Density Approximation (LDA) to DFT have provided a simple framework whose accuracy and predictive power have been convincingly demonstrated in a large variety of systems [24]. The calculation of reliable phonon spectra and other dynamical properties in real materials is well within the reach of DFT.

We will proceed now with the description of the computer package used in this work whose name is *ESPRESSO*. It is a modular tool in which each module or subprogram takes the responsibility for one part of the full characterization of the system. It is in this way that, for example, the module *pw.x* is the subprogram responsible of minimizing the ground state energy by finding the best possible ground-state electronic density $n_0(r)$ through the superposition of a limited basis set which is composed of a finite number of plane waves. Then, many other things can be done even in a non self consistent way. For example, using the ground state set of wave functions found after the minimization with *pw.x*, it is also possible (with the same module) to calculate the electronic energies for an arbitrary set of k-points of the reciprocal space and then construct a bands-diagram. One can use another subprogram, such as *ph.x*, that takes this same optimized set of plane waves, and use it to obtain the phonon frequencies at certain k-points, in order to construct the phonon dispersion curves associated with the system.

Another very interesting thing that we can do is to optimize the system's configuration. This is attained by using the so called relaxation mode within the subprogram *pw.x*, in which, one has to give arbitrary initial positions for the atoms as an input and then the program will try to evolve certain allowed-to-move parts of the system toward an equilibrium position, were the forces acting

[3] Or equivalently at *www.pwscf.org*

over each atom will be zero. This is particularly useful in our first problem, where there is an uncertainty about the position occupied by the nitrogens inside the *fcc* structure formed by the Platinum atoms.

The *pw.x* program, in general, will not perform the self-consistent energy minimizations over the entire Brillouin zone, but will use the available symmetries of the system to sample an smaller zone so that, the computational effort can be reduced as much as possible while sampling a representative portion of the reciprocal space. Among the most important parameters in the input file we have:

ibrav is the kind of Bravais lattice we are simulating, *ibrav=2* is for *fcc*.

celldm is the lattice parameter of the crystal and is usually given in Angstroms.

ecutwfc is the energy cutoff, which limits the amount of plane waves that the program will use.

k_points is the number of points in the reciprocal space that the program will sample (after symmetry considerations) and in which the self consistent minimization of the energy will be performed.

nat means *number of atoms* i.e. how many atoms we will have per unit cell. in our case we used $nat = 2$ for PtN and $nat = 3$ for PtN_2.

ntyp means *number of tomic species* i.e. how many kinds of atoms are involved, for example $ntyp = 2$.

ATOMIC_SPECIES is the section where we will have to put the symbol of the atoms, their masses and which are the the files containing the pseudopotentials.

ATOMIC_POSITIONS; is the section in which we are supposed to give the spatial distribution of the atoms. In this field during a relaxation process, it can also be specified which atoms we want to have fixed and which are free to move.

Finally, for the molecular dynamics simulations, the program *fpmd.x* (*cp.x* in latest versions) was used.

Chapter 4

Platinum dinitride

There has been considerable interest in the synthesis of new nitrides because of their technological and fundamental importance [25, 26] . Owing to it having one of the strongest covalent bonds, Nitrogen is very stable and inert under normal conditions. Yet Nitrogen reacts with selected elements, forming compounds with a variety of intriguing properties. Some of the nitrides (mostly of group III and IV elements) produced by various methods are widely used as optoelectronic materials for example, light-emitting diodes and semiconducting lasers. Theoretical studies of nitrides are also numerous, covering the topics of optoelectronics [27, 28], physical and structural properties [27, 29, 30] and superconductivity [31], the latter due to the fact that another important group of these materials is the transition metal nitrides mostly known for their superconducting properties [32, 33, 34, 35, 36], most of these transition metals form nitrides at high temperatures and at either ambient or high pressures (for example, ZrN, VN, MoN).

Although numerous metals react with Nitrogen, there were no binary nitrides known of the noble metals. Platinum in the other hand, forms simple binary compounds with halogens (for example, PtF_4, PtI_2); oxides and chalcogenides (for example, PtO, PtS) but it was not known to form crystalline nitrides [37], in fact, previously, only reactions forming small molecules containing Pt and N in the gas phase have been reported (diatomic PtN by sputtering [38] and PtN, PtN_2 and $(PtN)_2$ by laser ablation [39]).

As reported in by Eugene Gregoryanz *et al.* [2], the reaction between pure Platinum and Nitrogen was first observed in Raman measurements following laser heating of samples at 2000 K and at pressures above 45 GPa. At lower pressures, after numerous heatings, the transformation to the nitride phase was never observed, whereas above 45 - 50 GPa the transition proceeds rapidly. For us, this means that the transition takes place in a point where the pressure reaches a value in which the crystalline PtN compound is more stable than having a separated Pt crystal and N_2 molecules; and then the complete recovery of the product when quenched to ambient conditions as they report, would be due to hysteresis effects. This is confirmed by the finding (also reported by Gregoryanz in his paper) that the PtN compound breaks down when temperature is increased to around 450 K at ambient pressure.

4.1 Experimental characterization

The paper by Gregoryanz *et al.*. describes how they discover the presence of the new compound due to an in situ Raman spectroscopy which showed what seemed to be a new strong longitudinal optic (LO) mode and a weaker transverse optic (TO) mode (see Fig. 4.1) being this spectra similar to that of cubic GaN and InN, though the peaks are shifted in frequency as expected from mass effects [40, 41].

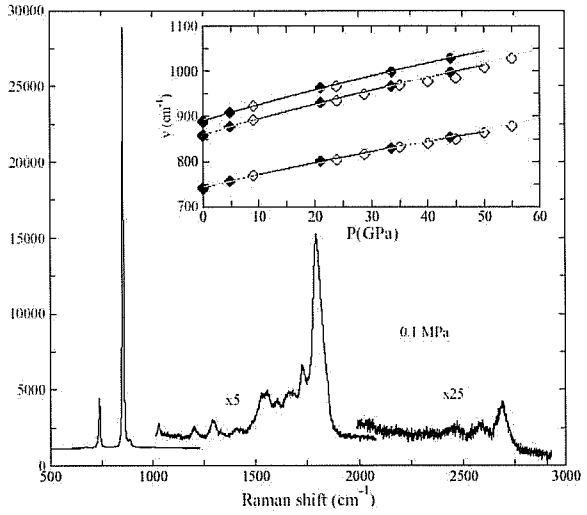

Figure 4.1: Raman spectra for the new compound.

After decompression, samples were recovered at ambient conditions and analyzed by electron microprobe. Compositional profiles showed that the Pt/N ratio is close to 1:1 but with some variations, pure Platinum remained on the borders of the sample and also to lesser degree in the bulk. The micro-Raman spectra measured across all PtN grains studied were identical, being this consistent with essentially no variation in stoichiometry and even more, the strength and width of the Raman fundamental bands are indicative of well-crystallized and highly ordered structure.

Multiple characterizations by synchrotron X-ray diffraction showed that all patterns, taken at different pressures, are consistent between them; and PtN can be indexed as *fcc* for all pressures (with lattice spacing $a = 4.8041(2)$ Å at 0.1 M Pa). Even though the Rietveld refinement demonstrated to be complicated by the strong Pt signal, the refinement agrees with the non-centrosymmetric space group $F\bar{4}3m$, to which the zinc-blende structure belongs, as well as the rocksalt structure. But even though it is true that the big mass difference between Pt and N makes it impossible to distinguish between the two structures mentioned above from the diffraction intensities, in principle the rocksalt structure can be discarded because it doesn't have a first-order Raman spectrum, while the

Quantity	*Experimental result*
Lattice parameter	4.8041(2) Å
Bulk modulus K_0	372(±5) GPa
$K_0\prime$	4.0
Phonons at Γ ($\pm 5\,cm^{-1}$)	745 — 865 — 895
Formation's pressure and temperature.	45-50 GPa at 2000 K
Conductivity	poor
Pt / N ratio	close to 1:1

Table 4.1: Experimental measurements for the new compound.

zinc-blende structure has two Raman active peaks which are more in agreement with the two strong first-order bands observed. However Gregoryanz notes in his paper the presence of some additional weaker peaks in the Raman spectra and some extra rings in the two-dimensional X-ray diffraction patterns, whose texture differs from both Pt and PtN rings. These inconsistencies are attributed by the author to residual non-stoichiometric material distributed throughout the sample.

The possibility of having a superconducting material was also tested using a magnetic susceptibility technique [42] and looking for the superconducting transition down to 2 K. No superconductivity was found, and this fact together with the visual appearance of PtN (lustrous and darker than pure Platinum in reflected white light, and totally opaque in transmitted light) suggests that the material should be either a poor metal or a semiconductor with a small bandgap.

Finally, two of the quantities that we were able to test by using DFT, are the zero-pressure bulk modulus K_0 which for this material seems to be very high, being of the order of 372(±5) GPa (about 100 GPa higher than the bulk modulus for pure Platinum); and its first derivative with respect to pressure, $K_0\prime = 4.0$. These results were obtained after fitting the evolution of the volume with pressure by means of a Birch-Murnaghan equation of state. Table 4.1 summarizes the experimental results mentioned in this section.

4.2 Ab-initio characterization

In this section we will show that according to our first-principles calculations, PtN_2 having pyrite structure is fully consistent with x-ray, Raman and compressibility measurements of Ref. [2]. Calculations [43] were performed within the density functional theory using a Perdew-Burke-Ernzerhoff exchange correlation functional [44] and a plane wave basis set for the electronic wave functions with a kinetic energy cut off of 60 Ry (80 Ry for phonon calculations). A pseudopotential description of the ion-electron interaction [45] was used, with platinum's $4s$ and $4p$ semicore states explicitly included in the valence. Brillouin zone integration was found to be converged with a uniform grid of $7 \times 7 \times 7$ points. Structural relaxations were limited to the nitrogen positions, with platinum atoms fixed on the fcc lattice and the experimental zero-pressure lattice

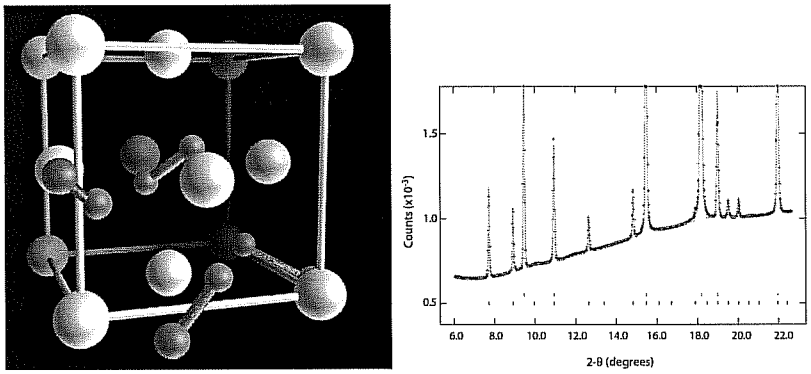

Figure 4.2: Left: Pyrite Structure of PtN_2, space group $P\bar{a}3$. Platinum atoms (white) form a face-centered cubic lattice, dinitrogen (N_2) units (blue) occupy the octahedral cavities of the Pt lattice. The calculated N-N distance at ambient pressure is 1.42 Å. Right: Rietveld fit using the $P\bar{a}3$ space-group. Red crosses: data at ambient pressure (λ=0.3738 Å); green line: Rietveld fit; black ticks: PtN_2 peaks; red ticks: Pt peaks. The most intense Pt peaks are cut off.

spacing (4.8041 Å). A preliminary search [46] on the minimal unit cell containing one PtN_2 formula unit (i.e. with the rhombohedral primitive unit cell of the fcc lattice) showed that a structure with an interstitial N_2 centered in the octahedral cavity of the Pt fcc lattice, gives an energy which is lower than that of all previously proposed structures, all of which are based on atomic nitrogen centered either on the octahedral cavities (rock salt) or on the tetrahedral cavities (zinc blende and fluorite). A single interstitial N_2, however, violates the cubic symmetry of the platinum sublattice and would lead to a sizeable rhombohedral distortion, which is not observed experimentally. In this work, a deeper energy minimum is obtained by expanding our analysis to the cubic conventional cell of the fcc metal lattice. Arranging the nitrogen atoms on the eightfold sites of space group $P\bar{a}3$ (see Fig. 1) minimizes the quadrupole interaction between the dinitrogen molecules, thus further reducing the energy, while preserving the observed cubic symmetry of the metal sublattice. The resulting pyrite isostructure agrees with all experimental data; indeed, a Reitveld refinement of the observed diffraction pattern using $P\bar{a}3$ (Fig. 1) is indistinguishable with experimental data as compared to the originally proposed zinc-blende structure. In this structure at ambient pressure, platinum atoms are accommodated on the Wyckoff site 4a and nitrogen atoms are on the site 8c with x=0.415.

PtN_2 pyrite is found to have a considerably lower ground state energy than that of any other proposed structures, rendering the existence of any of these phases of PtN or PtN_2 highly unlikely. Moreover, in contrast to the structures proposed in previous reports, the pyrite phase shows not only mechanical stability, but good agreement with both bulk properties and experimentally observed Raman spectra. Our calculations (see Table 1) show the pyrite structure to be 2 eV per stoichiometric unit lower in energy than the fluorite structure at ambient pressure. The comparison with 1:1 structures (zinc-blende and rocksalt) is based on their respective formation energies, and shows that pyrite has energy 0.3 eV (per Pt atom) lower than that of zinc-blende and 0.8 eV lower than

	a	B, B'	B, B'	ΔE (eV)
Exp.[2]	**4.804**	373, **4.00**	354, **5.23**	-
Pyr. (cal.)	4.848	305, **4.00**	285, 5.50	1.92
Fl. (cal.)	4.939	269, **4.00**	260, 4.73	3.95
ZB (cal.)	4.760	213, **4.00**	217, 3.62	2.20
RS (cal.)	4.471	251, **4.00**	242, 4.78	2.73
Pt exp.[47]	3.924	275, 4.78	277, 5.23	-
Pt cal.	3.966	242, 5.83	249, **5.23**	-

Table 4.2: Bulk modulus (in GPa), its pressure derivative (B'), and equilibrium lattice parameters (in Å), obtained from fitting calculated energies over a range of volumes with a second order Birch-Murnaghan equation of state. Bold values were fixed during fitting. Formation energies ΔE are relative to Pt+N_2 for PtN_2 compounds, Pt+$\frac{1}{2}N_2$ for PtN compounds.

that of rocksalt. The positive sign of the formation energies in our calculations reveal, however, that PtN_2 is unstable towards dissociation into its constituent elements, at least at zero pressure. This is corroborated by experimental evidence that, below 10 GPa, PtN_2 dissociates upon mild heating. The PtN_2 pyrite structure is characterized by Pt in six-fold coordination with N, with a calculated Pt-N distance of 2.096 Å at zero pressure. Each nitrogen is four-fold coordinated to three Pt atoms and one N atom. The interstitial dinitrogen unit has a zero-pressure N-N bond length of 1.42 Å , much longer than the molecular triple bond, and consistent instead with a N-N single bond. The calculated energy versus unit-cell volume was fitted with the Birch-Murnaghan equation of state, giving an equilibrium lattice parameter that agrees with experiment to within 1% (Table 1). The bulk modulus (B) is shown to be considerably higher than that of both bulk platinum and fluorite PtN_2, again in good agreement with experimental results. The slight overestimation of the lattice parameters and the underestimation of the calculated bulk moduli with respect to the experimental results, both for PtN_2 and for Pt, are a likely consequence of the choice of the PBE density functional[44].

In order to check the local mechanical stability of the pyrite structure we computed its elastic constants. For crystals with cubic symmetry, application of a single strain to the lattice vectors is sufficient to determine all three independent elastic constants [48]. These calculations –in addition to confirming the values of B calculated from the equations of state– also show pyrite structure PtN_2 to be mechanically stable and to have a relatively high shear modulus (Table 2), an important indicator for hardness in dielectrics [49]. The high G/B ratio (G being the shear modulus) or, equivalently, the low Poisson's ratio (ν) points to a high degree of covalency [50], suggesting that intercalation of the dinitrogen units into the Pt lattice induces a substantial change of the electronic structure from metallic, in bulk Pt, to covalent in PtN_2. Our elasticity calculations for zinc-blende PtN (Table 2) suggest that it is mechanically unstable, as claimed in [51], but our difference between c_{11} and c_{12} for that particular configuration is too small to allow us to make conclusive statements about stability within the approximations used. However, our calculations show conclusively that zinc-blende as well as rock-salt and fluorite structures are in

	c_{11}	c_{12}	c_{44}	B	G	E	ν
Pyrite	696	83	136	288	221	528	.19
Fluorite	473	160	115	264	136	348	.28
Zinc-Blende	197	200	22	199	10	30	.48
Rock-Salt	266	221	36	236	30	86	.44

Table 4.3: Elastic constants and elastic moduli in GPa for a variety of proposed PtN and PtN_2 phases, calculated in the limit of infinitesimal strain (E is the Young's modulus, other quantities are defined in the text). Mechanical stability for cubic crystals is expressed in the following conditions on the elastic constants [52]: $c_{44} > 0$, $c_{11} > |c_{12}|$, and $B = \frac{c_{11}+2c_{12}}{3} > 0$.

poor agreement with the bulk properties reported in Ref. [2] (Table 1).

The calculated zone-center vibrational modes of PtN_2 pyrite, as determined using density-functional perturbation theory [13], show good agreement with experimentally observed Raman spectra. Calculated and experimental Raman frequencies over a range of pressures are compared in Fig. 2a. Calculations show the existence of two almost degenerate modes giving rise to a Raman peak around 700 cm^{-1} (Fig. 2a) which was reported but not shown in [2] and originally attributed to a non-stoichiometry of the samples. The calculated Raman intensities [53] (Fig. 2b) show the presence of two intense peaks, in good agreement with the experimental results, and of three weak modes, two of which are seen in the experimental spectra. It is interesting to note that all Raman active phonon modes of PtN_2 pyrite, although calculated using the full cell, arise only from the displacements of the nitrogen atoms, and do not have Pt components. In fact their frequencies are in fair agreement with those predicted [54] and later observed [55] for single-bonded nitrogen in its polymeric phase.

Finally, the calculated electronic band structure of pyrite PtN_2 at zero pressure, reported in Fig. 3, shows a clear insulating character. Band gaps are typically underestimated within density functional theory, so the calculated indirect band gap of about 1.5 eV could correspond to a true gap of 2-3 eV, which would make PtN_2 an interesting candidate for optical applications [56]. The insulating character is consistent with the covalent nature of bonding revealed by the low Poisson's ratio.

All the evidences presented so far strongly indicate that the new compound has a $Pa\bar{3}$ structure with interstitial single-bonded N_2 units, hence making it desirable to find an explanation for how this structure can in effect be responsible for the hardness and insulating properties of this compound. Insertion of atomic nitrogen into transition metals is known to lead to an increase in directional bonding and therefore to an increase of mechanical strength. Grossman *et al.* [57] have shown that such changes are more dramatic for early transition metals, due to the fact that the flat density distribution of the elemental phase is more heavily altered by the insertion of interstitial nitrogen atoms. Late (heavier) transition metals have a more corrugated density distributions in their elemental phases, and therefore should not increase their hardness in the nitride phases, as shown in [57] for the rock salt phases. A histogram of the density distribution for pyrite PtN_2 (Fig. 4) shows however that insertion of dinitrogen in Pt causes a fourfold reduction of the histogram peak, which is qualitatively comparable to

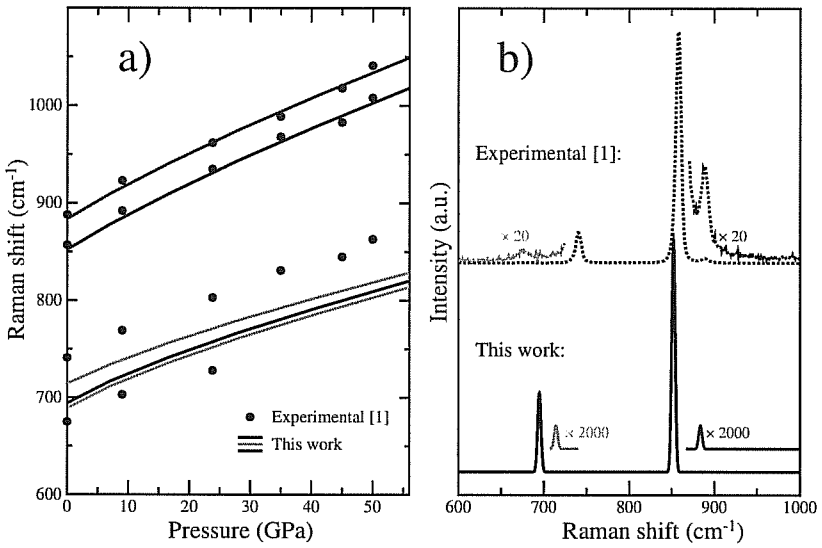

Figure 4.3: (a) Calculated and experimental (from Ref. 1) Raman frequencies as a function of pressure. An agreement within 5% in the frequency determination is typical for this kind of calculations. (b) Calculated and experimental Raman intensities. An additional calculated peak with intensity similar to the green peak at 710 cm^{-1} is not shown as its frequency overlaps with the intense mode at 695 cm^{-1}.

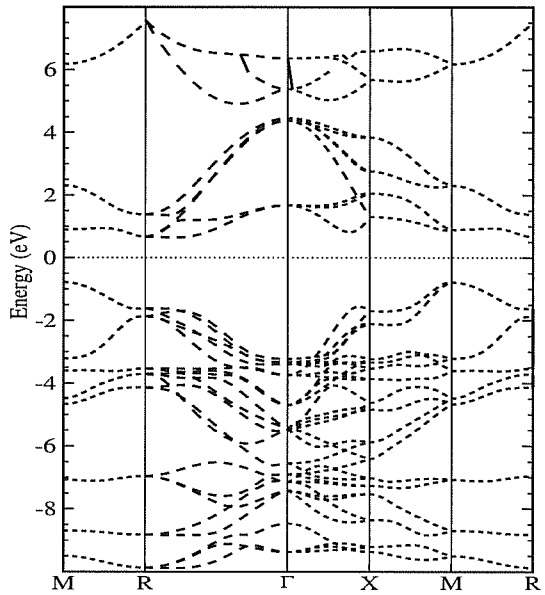

Figure 4.4: Electronic bands of Pyrite PtN_2 at ambient pressure along high symmetry directions. Filled states have negative energies.

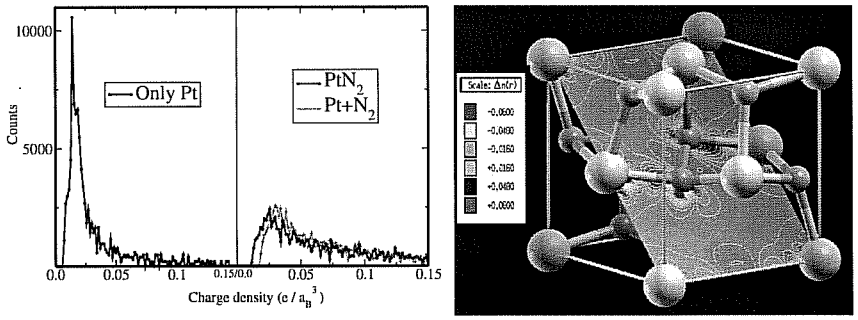

Figure 4.5: Left: Histogram of charge densities for bulk Pt (left), for PtN_2 (right, black), and for Pt+N_2 (right, red). Right: Cut of the charge density difference (compound – individual atoms) showing charge displacement.

the reduction observed in Ref. [57] for light transition metals, indicating that directional bonding with dinitrogen interstitials is stronger than with atomic nitrogen. Moreover, a comparison of the density histogram of PtN_2 with that obtained by summing the densities of Pt and N_2 calculated separately but at the same lattice positions, shows that, in the compound, the charge density reaches a lower minimum value than that obtained for the sum of the Pt and N_2 densities. This is also clear from Fig. 4, where a two-dimensional cut of such charge difference is shown. Besides a noticeable rehybridization of the Pt semicore orbitals, the figure also shows that, in the PtN_2 compound, charge flows from interstitial low-density regions to bonding regions of higher density, which is again consistent with covalency. The presence of interstitial dinitrogen units is crucial to explain the insulating character of pyrite PtN_2, since all platinum nitride structures proposed so far contain interstitial nitrogen in the atomic form and have been reported to be conducting.

In conclusion, in Ref. [2] platinum nitrite was observed as a result of the reaction of a molecular nitrogen fluid with Pt metal at high pressure and temperature (P $\sim$ 45 GPa and T$\sim$ 2000 K). Here, we show that this compound is PtN_2 having a pyrite structure consisting of interstitial single-bonded N_2 units incorporated in the octahedral cavities of a fcc Pt sub-lattice. This incorporation implies a change of bonding for N_2 from triple to single, a transition that molecular nitrogen is known to undergo during amorphization at similar pressures [58]. We therefore argue that pressure-induced changes in the bonding character of nitrogen are key to understand the synthesis of PtN_2.

Chapter 5

Carbon dioxide

CO_2 is very stable and very abundant since it is a final residua of many reactions. So, it contributes to increase the pollution problem and green-house effect, then it would be desirable to device a method for storing CO_2 in a environmental friendly fashion. There has been an active research in its phase diagram , but since the C-O bond in carbon is very strong most of the solid phases we know for this material are of the molecular kind. One of the most desirable solutions would be the one consisting on bringing the CO_2 to a phase similar to those that exist for SiO_2, in order to make it stable so it will continue being solid under normal conditions and this will make possible to get advantages from its possible technological uses.

5.1 CO_2's polymeric phase

As described above, CO_2 is also very stable and its polymeric phase is, in our study, a target state which we would like to reach at more reasonable conditions than the ones proposed up to now. Here ab-initio is used for testing some physically and chemically grounded ideas.
About the polymeric phase we know that it may be an ultra-hard material. Science, 284, 788 (1999) and it has been already synthesized in laboratory under extreme conditions (T=1800 K, P=40 GPa.) Science, 283, 1510 (1999). We also know that a possible intermediate in this process at high T and P is a C_2O_4 ring (Tassone et al, Chem. Phys. Chem., 6, 1752 (2005) which are very stable structures and have to be avoided in order to reach a real long range polymeric phase.
Our idea is to dope the molecular CO_2 with titanium, but instead of doing this by setting an expensive experiment we will use the Ab-initio MD technique to simulate a box containing 50 CO_2 molecules + 1 Ti $(C_2O_4)_2$ complex and hence discover if this transition metal can suppress the ring formation and activate the C-O bond in order to initiate the polymerization at lower tmperature.
Our Ab-initio code uses PBE exchange and correlation, Martin-Trouiller pseudo-potentials an plain-waves' energy cut off = 90 Ry. The MD program runs with a constant pressure algorithm that can be set from the input to reach the desired pressure since the program can tune the geometry of the cell by applying the variable cell (Parinello-Raman) technique. Our preliminary results suggest that

transition metal complexes of Ti may be used to initiate CO_2 polymerization at ambient temperatures and lower pressures than pure CO_2. Beyond completion of this study we can also consider further extending this paradigm to other systems, for example to the N_2 polymerization.

Chapter 6

Conclusions

In this project we were not only testing the DFT technique by comparing our results with already known ones (we did this in *chapter 4* for Pt and N_2 elements), but also doing some research effort so that, we were able to find good clues about some unanswered questions. One of the main conclusions of this work is that, trusting in a well tested and reliable program as pw.x and ph.x inside *ESPRESSO*, we can disregard (at least from the DFT-within-LDA's point of view) the experimentally suggested zinc-blende and rocksalt structures as the actual ones for the recently discovered Platinum-nitride compound. These two structures in spite of being the options preferred by the experimental group who synthesize the compound are in a very high disagreement with their own experimental data, while we found that PtN_2 with pyrite structure, is a configuration much more suitable to explain the observed behavior.

Finally, we are confident about the future of our runs with CO_2 since, as we saw, the first part of the polymerization process has been achieved.

Bibliography

[1] N. Meskini and K. Kunc. Technical Report 5, Université P. et M. Curie, 1978. unpublished.

[2] M. Somayazulu J. Badro G. Fiquet H. K. Mao E. Gregoryanz, C. Sanloup and R. J. Hemley. *Nature-materials*, **3**:294–297, 2004.

[3] Pasquale Pavone. *Lattice Dynamics of Semiconductors from Density-Functional Perturbation Theory.* PhD thesis, SISSA - Trieste, IT., 1991.

[4] M. Born and J. R. Oppenheimer. *Ann. Phys. (Leipzig)*, **84**:457, 1927.

[5] P.D. De Cicco and F.A. Johnson. *Proc. R. Soc. London Ser.*, **A 310**:111, 1969.

[6] M.H. Cohen R. Pick and R.M. Martin. *Phys. Rev B*, **1**:910, 1970.

[7] P. Hohenberg and W. Kohn. *Phys. Rev.*, **136**:B864–871, 1964.

[8] N. D. Mermin. *Phys. Rev.*, **137**:A1441–1443, 1965.

[9] W. Kohn and L. J. Sham. *Phys. Rev.*, **140**:A1133–1138, 1965.

[10] R.M. Martin. *Electronic structure: basic theory and practical methods.* Cambridge, University Press, 2004.

[11] H. Hellman. *Deuticke, Leipzig*, 1937.

[12] R.P. Feynman. *Phys. Rev.*, **56**:340, 1939.

[13] A. dal Corso S. Baroni, S. de Gironcolli and P. Giannozzi. *Rev. Mod. Phys*, **73**(2):515–562, 2001.

[14] R.G Parr and W. Yang. *Density Functional Theory of Atoms and Molecules.* Oxford University Press, N.Y, 1989.

[15] R.M. Dreizler and E.K.U. Gross. *Density Functional Theory.* Springer, Berlin, 1990.

[16] Andrea Dal Corso. *Density Functional Theory beyond the pseudopotencial local density approach: a few cases studies.* PhD thesis, SISSA - Trieste, IT., October 1993.

[17] Alessandro Laio. *Simulation of Iron at Earths Core Conditions.* PhD thesis, SISSA - Trieste, IT., October 1999.

[18] Violeta Marinova Koratova. Ab-initio study of neutral and charged selenium chains. Diploma Thesis, I.C.T.P - Trieste, IT., 1996.

[19] Nguyen Hoang Phuong. Ab-initio spin polarized study of the ideal α-sn (111) surface, September. Diploma Thesis, I.C.T.P - Trieste, IT., 1998.

[20] D.R Hamann J.B. Bachelet and M. Schlüter. *Phys. Rev. B*, **26**:4199, 1982.

[21] M. Schlüter D.R Hamann and C. Chiang. *Phys. Rev. Lett*, **43**:1494, 1979.

[22] U. Von Barth and R. Car. unpublished.

[23] G.B. Bachelet and N.E Christensen. *Phys. Rev. B*, **31**:879, 1985.

[24] W.E. Pickett. *Comput. Phys. Rep*, **9**:115, 1989.

[25] P.F. MacMillan. *Nature Materials*, **1**:19–25, 2003.

[26] G. Miehe A. Zerr and R. Boehler. *Nature*, **400**:340–342, 1999.

[27] L. Ouyang P. Rulis I. Tanaka W. Ching, S. Mo and M. Yoshiya. *J. Am. Ceram. Soc*, **85**:78–80, 2002.

[28] S.K. Deb G. Wolf J. Dong, O.F. Sankey and P.F. MacMillan. *Phys. Rev. B*, **61**:11979–11992, 2000.

[29] P. Kroll. *Phys. Rev. Lett.*, **90**:125501, 2003.

[30] L. Ouyang I. Tanaka W.Y. Ching, S. Mo and M. Yoshiya. *Phys. Rev. B*, **61**:10609–10614, 2000.

[31] B.M. Klein D.A. Papaconstantopoulos, W.E. Pickett and L.L. Boyer. *Phys. Rev. B*, **31**:752–761, 1985.

[32] R.E. Gold N. Pessal and W.A. Reichardt. *J. Phys. Chem. Solids*, **29**:19–38, 1968.

[33] H. Pierson. *Handbook of Refractory Carbides and Nitrides: Properties, Characteristics and Applications.* Noyes Publications, Westwood, N.J., (1996).

[34] W. Fuller A.S. Edelstein H.L. Luo, S.A. Wolf and C.Y. Huang. *Phys. Rev. B*, **29**:1443–1446, 1984.

[35] G. Rubino K.E. Grey J. Zasadzinsky, R. Vaglio and M. Russo. *Phys. Rev. B*, **32**:2929–2934, 1985.

[36] D.B. Dove R.W. Nywening T. Takamori, K.K. Shih and M.E. Re. *j. Appl. Phys*, **68**:2192–2195, 1990.

[37] N. Greenwood and A. Earnshaw. *Chemistry of the Elements.* Butterworth-Heinemann, 1997.

[38] E. J. Friedman-Hill and R.W. Field. *j. Chem. Phys.*, **100**:6141–6152, 1994.

[39] W.D. Bare A. Cintra, X. Wang and L. Andrews. *j. Chem. Phys. A*, **105**:7799–7811, 2001.

[40] K. Syassen C. Thomsen A.R. Goñi, H. Siegle and J.M. Wagner. *phys. Rev. B*, **64**:35205, 2001.

[41] A. Tabata et al. *Appl. Phys. Lett.*, **74**, 1999.

[42] R.J. Hemley H.K. Mao Y. Timofeev, V.V. Struzhkin and E.A. Gregoryanz. *Rev. Sci. Instrum*, **73**:371–377, 2002.

[43] `http://www.quantum-espresso.org`.

[44] K. Burke J. Perdew and M. Ernzerhof. *Phys. Rev. Lett.*, **77**:3865, 1996.

[45] D. Vanderbilt. *Phys. Rev. B*, **41**:7892, 1990.

[46] J. A. Montoya. *Diploma Thesis, ICTP, Trieste-Italy*, 2004.

[47] P. Loubeyre A. Dewaele and M. Mezouar. *Phys. Rev. B*, **70**:094112, 2004.

[48] B. B. Karki *et al. Amer. Mineral.*, **82**:51, 1997.

[49] J. M. Leger *et al. Appl. Phys. Lett.*, **79**:2169, 2001.

[50] A. G. Lyapin V. V. Brazhkin and R. J. Hemley. *Phil. Mag. A*, **82**:231, 2002.

[51] R. Yu and X. F. Zhang. *Appl. Phys. Lett.*, **86**:121913, 2005.

[52] J. F. Nye. *Physical Properties of Crystals*. Oxford University Press, Oxford, (1985).

[53] M. Lazzeri and F. Mauri. *Phys. Rev. Lett.*, **90**:036401, 2003.

[54] T. W. Barbee III. *Phys. Rev. B*, **48**:9327, 1993.

[55] M. I. Eremets *et al. Nature Materials*, **3**:558, 2004.

[56] P. F. McMillan. *Nature Materials*, **1**:19, 2003.

[57] J. Grossman *et al. Phys. Rev. B*, **60**:6343–6347, 1999.

[58] R.J. Hemley E. Gregoryanz, A. Goncharov and H. k. Mao. *Phys. Rev. B*, **64**:052103, 2001.